# Numerical investigation of all-optical add-drop multiplexing for spectrally overlapping OFDM signals

**S. Sygletos,[1,*] S. Fabbri,[1,2] E. Giacoumidis,[1] M. Sorokina,[1] D. M. Marom,[3] M.F.C. Stephens,[1] D. Klonidis,[4] I. Tomkos,[4] and A. D. Ellis[1]**

[1]*Aston Institute of Photonic Technologies, Aston University, Birmingham, UK*
[2]*Department of Physics, University College Cork, Ireland*
[3]*Department of Applied Physics, Hebrew University, Jerusalem, Israel*
[4]*Athens Information Technology Center, Athens, Greece*

[*]*s.sygletos@aston.ac.uk*

**Abstract:** We propose a novel architecture for all-optical add-drop multiplexing of OFDM signals. Sub-channel extraction is achieved by means of waveform replication and coherent subtraction from the OFDM super-channel. Numerical simulations have been carried out to benchmark the performance of the architecture against critical design parameters.



**OCIS codes:** (060.1155) All-optical networks; (060.1660) Coherent communications.

## References and links

1. I.Tomkos, M. Vasilyev, J. Rhee, M. Mehendale, B. Hallock, B. Szalabofka, M. Williams, S. Tsuda, and M. Sharma,"80x10.7 Gb/s Ultra-Long-Haul(+4200 km) DWDM network with reconfigurable "Broadcast & Select" OADMs," in Optical Fiber Communications Conference, A. Sawchuk, ed., Vol. 70 of OSA Trends in Optics and Photonics (Optical Society of America, 2002), paper FC1.
2. S. Sygletos, I. Tomkos, and J. Leuthold, "Technological challenges on the road toward transparent networking," J. Opt. Netw. **7**(4), 321–350 (2008).
3. A. D. Ellis and F. C. Gunning, "Spectral density enhancement using coherent WDM," IEEE Photon. Technol. Lett. **15**(2), 504–506 (2005).
4. A. Sano, E. Yamada, H. Masuda, E. Yamazaki, T. Kobayashi, E. Yoshida, Y. Miyamoto, R. Kudo, K. Ishihara, and Y. Takatori, "No-guard-interval coherent optical OFDM for 100 Gb/s long-haul WDM transmission," IEEE J. Lightw. Technol. **27**(16), 3705–3713 (2009).
5. G. Bosco, V. Curri, A. Carena, P. Poggiolini, and F. Forghieri, "On the performance of Nyquist-WDM terabit superchannels based on PM-BPSK, PM-QPSK, PM-8QAM or PM-16QAM Sub-carriers," IEEE J. Lightw. Technol. **29**(1), 53–61 (2011).
6. R. Schmogrow, M. Winter, M. Meyer, D. Hillerkuss, S. Wolf, B. Baeuerle, A. Ludwig, B. Nebendahl, S. Ben-Ezra, J. Meyer, M. Dreschmann, M. Huebner, J. Becker, C. Koos, W. Freude, and J. Leuthold, "Real-time Nyquist pulse generation beyond 100 Gbit/s and its relation to OFDM," Opt. Express **20**(1), 317–337 (2012).
7. E. Pincemin, M. Song, J. Karaki, O. Zia-Chahabi, T. Guilossou, D. Grot, G. Thouenon, C. Betoule, R. Clavier, A. Poudoulec, M. Van der Keur, Y. Jaouen, R. Le Bidan, T. Le Gall, P. Gravey, M. Morvan, B. Dumas-Feris, M. L. Moulinard, and G. Froc, "Multi-band OFDM transmission at 100 Gbps with sub-band optical switching," IEEE J. Lightw. Technol. **32**(12), 2202–2219 (2014).
8. M. G. Taylor, "Coherent optical channel substitution," Patent No. 8,050,564,(2011).
9. P. Winzer, "An opto-electronic interferometer and its use in sub-carrier add/drop multiplexing," IEEE J. Lightw. Technol. **31**(11), 1775–1782 (2013).
10. T. Richter, C. Schmidt-Langhorst, R. Elschner, T. Kato, T. Tanimura, S. Watanabe, and C. Schubert, "Coherent in-line substitution of OFDM subcarriers using fiber-frequency conversion and free-running lasers," in Optical Fiber Communication Conference: Postdeadline Papers, (Optical Society of America, 2014), paper Th5B.6.
11. D. Hillerkuss, M. Winter, M. Teschke, A. Marculescu, J. Li, G. Sigurdsson, K. Worms, S. Ben Ezra, N. Narkiss, W. Freude, and J. Leuthold, "Simple all-optical FFT scheme enabling Tbit/s real time signal processing," Opt. Express **18**(9), 9324–9340 (2010).

#227008 - $15.00 USD Received 17 Nov 2014; revised 11 Feb 2015; accepted 11 Feb 2015; published 25 Feb 2015

12. A. J. Lowery,"Design of arrayed-waveguide grating routers for use as an optical OFDM demultiplexers," Opt. Express **18**(13), 14129–14143 (2010).
13. S. Frisken, G. Baxter, D. Abakoumov, H. Zhou, I. Clarke, and S. Poole, "Flexible and grid-less wavelength selective switch using LCOS technology," in Optical Fiber Communication Conference/National Fiber Optic Engineers Conference 2011, OSA Technical Digest (CD) (Optical Society of America, 2011), paper OTuM3.
14. M. J. Power, W. Jia, R. P. Webb, R. J. Manning, and F. C. Garcia Gunning,"Four-wave mixing for clock recovery of phase modulated optical OFDM super-channel," Opt. Express **22**(6), 7007–7013 (2014).
15. S. Kodama, T. Ito, N. Watanabase, S. Kondo, H. Takeuchi, H. Ito, and T. Ishibashi, "2.3 picoseconds optical gate monolithically integrating photodiode and electro-absorption modulator," Electron. Lett. **37**(19), 1185–1186 (2001).
16. K. E. Stubkjaer, "Semiconductor optical amplifier-based all-optical gates for high speed optical processing," IEEE J. Select. Topics in Quantum Electr. **6**(6), 1428–1435 (2000).
17. A. D. Ellis, T. Widdowson, X. Shan and D. G. Moodie, "Three-node, 40Gbit/s OTDM network experiment using electro-optic switches," Elecron. Lett. **30**(15), 1333–1334 (1994).
18. R. Slavik, J. Kakande, D. J. Richardson, "Feed-forward true carrier extraction of high baud rate phase shift keyed signals using photonic modulation stripping and low-bandwidth electronics," Opt. Express **19**(27), 26594–26599 (2011).
19. S. K. Ibrahim, S. Sygletos, R. Weerasuriya, and A. D. Ellis, "Novel real-time homodyne coherent receiver using a feed-forward based carrier extraction scheme for phase modulated signals," Opt. Express **19**(9), 8320–8326 (2011).
20. A. C. Bordonalli, C. Walton, A. J. Seeds, "High-performance locking of wide linewidth semiconductor lasers by combined use of optical injection locking and optical phase-lock loop," J. Lightw. Technol. **17**(2), 328–342 (1999).
21. A. Naka, T. Matsuda, S. Saito, "Receiver performance analysis and basic design for optical time-division multiplexed transmission systems," Electronics and Communications in Japan, Part 1 **83**(4), 93–104 (2000).
22. S. K. Ibrahim, J. Zhao, F. G. Gunning, P. Frascella, F. H. Peters, and A. D. Ellis, "Towards a practical implementation of coherent WDM: Analytical, Numerical and Experimental Studies," IEEE Photonics Journal **2**(5), 833–847 (2010).
23. D. Sinefeld, D. M . Marom, "Hybrid guided-wave/free-space optics photonic spectral processor based on LcoS phase only modulator," IEEE Photon. Technol. Lett. **22**(7), 510–512 (2010).
24. D. Sinefeld, S. Ben-Ezra, D. Marom, "Nyquist-WDM filter shaping with a high-resolution colorless photonic spectral processor," Opt. Letters **38**(17), 3268–3271 (2013).
25. D. M. Marom, D. T. Neilson, D. S. Greywall, C. S. Pai, N. R. Basavanhally, V. A. Aksyuk, D. O. Lopez, F. Pardo, M. E. Simon, Y. Low, P. Kolodner, and C. A. Bolle, "Wavelength-selective 1xK switches using free-space optics and MEMS micromirrors: theory, design, and implementation," IEEE J. Lightwave Technol. **23**(4), 1620–1630 (2005).
26. J.-C Antona, E. Grellier, A. Bononi, S. Petitrenaud, and S. Bigo, "Revisiting binary sequence length requirements for the accurate estimation of highly dispersive transmission systems," in Proc. ECOC 2008 (Brussels, Belgium, 2008), paper We.1.E.3.
27. M. C. Jeruchim, "Techniques for estimating the bit error rate in the simulation of digital communication systems," IEEE J. Selec. Areas Commun. **2**(1), 153–170 (1984).
28. R. Rudnick, A. Tolmachev, D. Sinefeld, O. Golani, S. Ben-Ezra, M. Nazarathy, D. Marom, "Sub-banded/single-sub-carrier drop-demux and flexible spectral shaping with a fine resolution photonic processor." in Proc. ECOC 2014 (Cannes, France), paper PD.4.1.

## 1. Introduction

The development of reconfigurable add-drop multiplexers (R-OADMs) and optical cross-connects had a dramatic impact on the evolution of transparent networking. They introduced the concepts of all-optical bypassing and dynamic wavelength routing, which relieved the nodes from the electronic processing of the through traffic and enabled dynamic allocation of the system capacity according to the evolving network needs [1, 2]. Currently, the switching functionality of R-OADM architectures is based on the use of wavelength selective switches (WSS), which route the dropped WDM channels to receivers and create empty spectral slots for new signals to be added. The specific approach is transparent to modulation format and capable of dealing with dense wavelength division multiplexing (DWDM) schemes. However, the recent introduction of highly spectral efficient multiplexing in optical transmission, such as the orthogonal frequency division multiplexing (OFDM) [3, 4] and the Nyquist-WDM [5, 6],which achieved reduction of the channel spacing down to the Nyquist rate, has set more stringent

#227008 - $15.00 USD Received 17 Nov 2014; revised 11 Feb 2015; accepted 11 Feb 2015; published 25 Feb 2015

requirements in the performance of the wavelength blocking and selection processes. Whilst some progress has been made towards this goal by allowing spectral guard bands between multi-banded OFDM signals [7] for all-optical OFDM signals, where there is spectral overlapping of the sub-channels, such conventional R-OADM technologies are unable to perform switching without violating the signal orthogonality condition that ensures crosstalk free performance.

Recently, Taylor in [8] introduced a new method for removing a WDM channel and adding a new one in its place, based on the use of an optoelectronic interferometer structure and digital coherent detection. Winzer in [9] proved, through numerical simulations, that a similar interferometric approach could be applicable also for Nyquist or OFDM signals provided that the orthogonality among the sub-channels is maintained through pulse reshaping in the digital domain. However, the optoelectronic character of the solution sets major limitations in terms of power consumption and interferometer stability due to the latency in the digital path. Formation of an equivalent interferometer using nonlinear optics and pilot signals for channel erasure has been demonstrated recently in a back to back configuration [10], however in addition to the obvious power consumption challenges of the required nonlinear optics, the local generation of the channel replica has yet to be established.

In this paper, we propose a novel all-optical approach to enable add-drop multiplexing of OFDM signals in the optical domain without use of optoelectronic conversion and digital signal processing. Combining purely linear all-optical methods such as FFT filtering [11, 12], time-domain sampling and subsequent i-FFT filtering, we create a replica of the sub-channel waveform and achieve its extraction from the original OFDM super-channel by coherent superposition. The node is completed using a simple coherent insertion process where appropriate frequency locking is based on established carrier extraction techniques. Through an in depth numerical study of its performance we have identified the main sources of degradation and optimized critical subsystem parameters resulting in penalties of less than 0.5 dB for the complete set of insert, drop and extract operations, which is dominated by component insertion losses.

## 2. Description of proposed ROADM architecture

The ROADM architecture is depicted in Fig 1(a) (the central schematic). Two conventional Wavelength Selective Switch (WSSs) units, one at the input and one at the output of the node, perform the selection of the super-channel, and after its processing, the re-insertion back into the network. The WSSs should have a capability for grid-less operation [13]. Within the super-channel to be processed, sub-channel switching is achieved by means of a three branch interferometer structure (branches labelled A, B, C for convenience). The architecture is modular in the sense that additional interferometer sub paths can be connected in parallel using the available WSS ports to increase the number of super-channels that can be simultaneously processed by the node.

At each interferometer, the selected super-channel is divided into three copies, one copy is dropped to the local receivers of the node and the two remaining copies feed interferometer branches A and B. Sub-channel blocking is facilitated by replicating the corresponding signal waveform in branch B and interfering it destructively with the super-channel that propagates through branch A. During the channel replication process, the signals remain purely in the optical domain and they are processed in the following three stages. The first stage involves demultiplexing of the OFDM signal, by an optical Fast Fourier Transform (FFT) processor [11, 12]. Subsequently, a bank of optical gates (one for each sub-channel to be extracted) performs time sampling of the sub-channels that need to be blocked from the through path. The optical gates are synchronized to a common clock signal extracted from the super-channel receivers (drop path) [14]. To illustrate the process, Fig. 1(b) depicts the simulated optical spectrum of

#227008 - $15.00 USD Received 17 Nov 2014; revised 11 Feb 2015; accepted 11 Feb 2015; published 25 Feb 2015

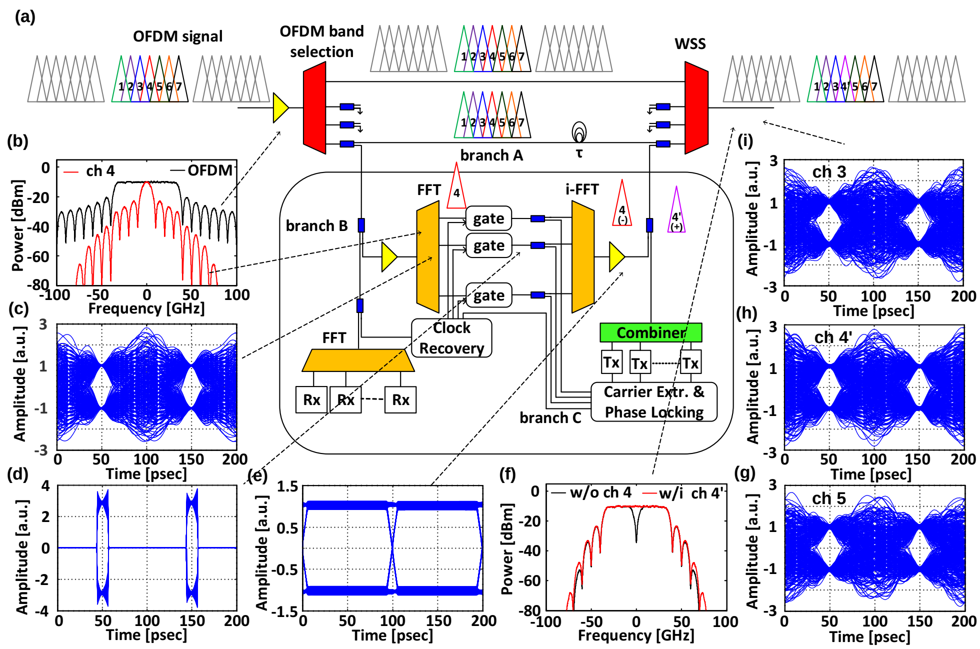

Fig. 1. (a) Diagram of proposed optical add-drop multiplexer for OFDM signals; (b) Optical spectrum of input OFDM super-channel (black), and of middle sub-channel after FFT de-multiplexing (red); (c) corresponding eye diagram of de-multiplexed signal; (d) eye-diagram of the sampled signal; (e) eye-diagram after the shaping of the i-FFT filter; (f) optical spectrum of the OFDM super-channel at the output of the node when the middle channel (ch 4) has been removed (black) and a new one (ch 4′) has taken its place (red); (g) eye-diagram of ch 5 at the output of the node; (h) eye-diagram of ch 4′ at the output of the node; (i) eye-diagram of ch 3 at the output of the node.

an OFDM signal (black), consisting of 7 BPSK sub-carriers, at the input of the node, before the WSS selection. The optical spectrum of the middle (ch 4) sub-channel after the FFT de-multiplexing is also shown in the same figure (red). The corresponding eye-diagram of ch 4, see Fig. 1(c), has reduced phase margin due to the preceding matched filtering and the inter-symbol interference (ISI) from the neighboring channels. In this example completely crosstalk free regions cannot be identified, as the orthogonality condition has been violated due to the tight pass-band filtering in the WSS and the finite bandwidth of the transmitter. By the insertion of a guard interval, long enough to contain the inter-symbol transitions, a crosstalk free observation window can be created at cost of a slightly reduced symbol rate.

Optical sampling [15–17] is performed on the sub-channels that need to be extracted from the through path (e.g. ch 4). The gate selects a waveform window of minimum crosstalk, see Fig. 1(d), and feeds it to an optical i-FFT processor, with transfer function $H(f) = \mathrm{sinc}(fT)$, which will reshape the pulses back to their initial symbol duration $T$, see Fig. 1(e). The recovered waveform will be amplified and subsequently destructively interfered with the OFDM signal in branch A. From this process a spectral hole will be created leaving an empty position for the new channel to be inserted, see Fig. 1(f). The losses, optical delays and relative optical phases should be carefully adjusted to maximize the extinction of the extracted channel, with the same precision as shown in [9]. The insertion of the new channels takes place on a separate

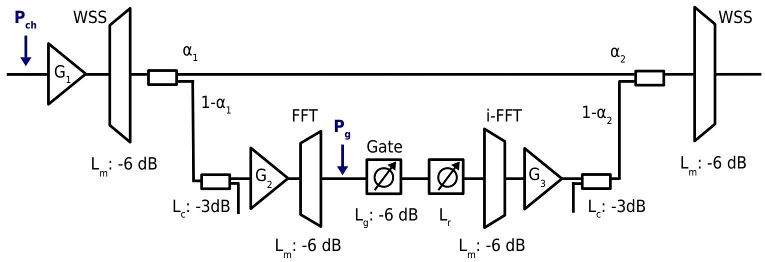


Fig. 2. Simplified diagram of proposed interferometric scheme depicting the loss and gain factors of the various components for performing the power budgeting and the calculation of the signal to noise ratio performance

branch (i.e. branch C), with a bank of laser transmitters that are time and frequency aligned to the sub-channels of the OFDM signal, so to form a new OFDM super-channel. For the frequency/phase alignment of the inserted channel well known optical carrier extraction [18, 19] and phase locking methods [20] can be applied, whereas the time synchronization can be achieved with the same clock signal that is used for the sampling process. The resulting optical spectrum, shown as the red trace in Fig. 1(f), and the clear eye diagrams of the added channel, see Fig. 1(h), and of its closest neighbours, i.e. ch 3 and ch 5 are shown in Fig. 1(g) and 1(i), confirm the successful add-drop operation of the proposed scheme.

## 3. Results and discussions

The goal of our study was to investigate the physical limitations of the proposed architecture and to specify the optimum parameters of the associated devices and subsystems. This has been achieved by decoupling the various sources of degradation and enabling separate calculation of their relative influence on the overall BER performance. As main degradation sources within the node, we have identified the amplified spontaneous emitted (ASE) noise from the erbium doped fiber amplifiers (EDFAs), the incomplete FFT/i-FFT processing due to the limited resolution of the optical filters and the incomplete sampling of the optical gate. Ideal phase synchronization of the local laser transmitters is considered, thus no additional phase errors are introduced during the sub-channel addition process.

### *3.1. Analysis of OSNR performance*

As it forms the critical path, we calculated the optical signal to noise ratio (OSNR) performance for the drop and extract operation. For this, we considered the insertion losses of our proposed configuration as depicted in Fig. 2. At the input of the node an average sub-channel signal power of $P_{ch}$ was assumed. The signal was boosted by the input amplifier, of gain $G_1$, which compensated the losses of the through path (branch A) from the two flex-grid WSS units and the two power couplers of the interferometer to give a lossless node. In the parallel path (branch B), the two amplifiers of gains $G_2$ and $G_3$ compensated for the corresponding losses, where we assumed a maximum input power to the optical gate, $P_g$, and common amplification in the case that multiple sub-channels are processed simultaneously. Electro-optic switches based on lithium niobate Mach Zehnder modulators [17] can tolerate mean input powers levels between 10 and 20 dBm, whereas optical gates based on semiconductor optical amplifiers [16] or electro-absorption [15] are strongly influenced by photocurrent when the signal power exceeds $\sim$0 dBm at their input. Apart from the optical losses $L_g$ of the gating device, the optical sampling and the i-FFT induced pulse reshaping processes introduced an excess loss factor $L_r$ in the

#227008 - $15.00 USD Received 17 Nov 2014; revised 11 Feb 2015; accepted 11 Feb 2015; published 25 Feb 2015

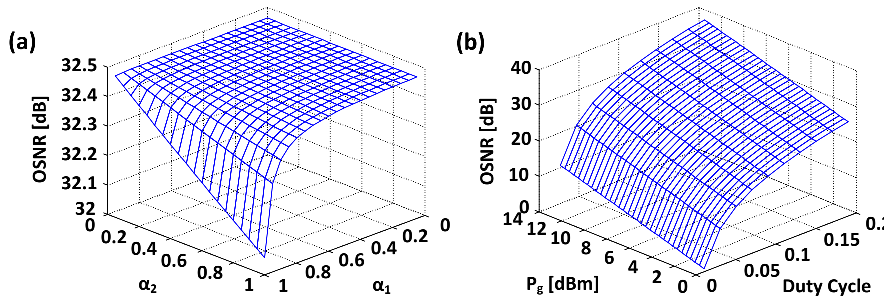


Fig. 3. (a) OSNR at the output of the node as a function of the power splitting rations $\alpha_1$,$\alpha_2$ of the input-output couplers of the interferometer ($P_g = 10\,\mathrm{dBm}, d = 0.12$); (b) OSNR at the output of the node as a function of the duty cycle $d$ and the launched power $P_g$ at the input of the gate ($\alpha_1$,$\alpha_2$=0.5)

parallel path, that scaled proportionally to the square of the gate duty cycle $d$ (i.e. $L_r = d^2$) [21], where the duty cycle was defined by the ratio of the switching window $sw$ to the bit duration $T$ (i.e. $d = sw/T$). Thus, a switching window of 10 ps, used to sample OFDM sub-channels of 10 Gbit/s, corresponded to 20 dB of extra losses. These had to be compensated by the subsequent amplifier, of gain $G_3$,which equalized the signal power to the level of branch A. However, this imposed a significant performance trade-off, i.e. short switching windows benefited the robustness of the system against inter-channel crosstalk, but at the expense of an increased OSNR degradation. The optimization steps of the following paragraphs helped us to reveal the relative influence of each effect and to identify the optimum operating point.

Based on the above power budget analysis we could easily define the gains of the three amplifiers as a function of the introduced losses within the node and of the sub-channel power levels $P_{ch}$ and $P_g$, i.e.

$$G_1 = \frac{1}{L_m^2 \alpha_1 \alpha_2}, \qquad G_2 = \frac{P_g}{P_{ch}} \frac{\alpha_1 \alpha_2}{(1-\alpha_1)L_c}, \qquad G_3 = \frac{P_{ch}}{P_g} \frac{1}{L_m^2 L_r L_g L_c (1-\alpha_2)} \tag{1}$$

Subsequently, an analytical expression was derived for the OSNR taking into account the ASE noise contributed from both interferometric branches A and B:

$$OSNR = \frac{P_{ch}}{NF h\nu B_0 \left[ 2G_1/(G_1-1) + \frac{P_{ch}}{P_g}(G_2-1)L_m + (G_3-1)(1-\alpha_2)L_c L_m \right]} \tag{2}$$

where $NF$ is the common noise figure of the three amplifiers, which in our case equals 5 dB, $B_0$ is the reference optical bandwidth of 12.5 GHz, $h$ is the Planck's constant and $\nu$ the optical frequency.

Figure 3(a) shows the analytically calculated OSNR at the output of the node, according to Eg. (1), Eq. (2), as a function the power spiting ratios $\alpha_1$,$\alpha_2$ of the input-output interferometric couplers, which ranged between 0 and 0.95. For the results we had assumed ideal signal at the input of the node (i.e. not degraded by ASE) with a sub-channel power level $P_{ch}$ of 0 dBm (and $P_g$ of 10 dBm). The duty cycle of the switching window was $d = 0.12$, which corresponded to 12 ps duration for the 100 ps symbol period of our proposed system. The graph shows a calculated OSNR performance of 32.47 dB with little dependence on the two power splitting parameters, except in the extreme case that there is negligible power directed towards branch B. This is because the OSNR is primarily degraded by the limited gate input power and the

#227008 - $15.00 USD Received 17 Nov 2014; revised 11 Feb 2015; accepted 11 Feb 2015; published 25 Feb 2015

effective loss of the combined gating and i-FFT filtering actions that take place in the parallel path. Consequently, $\alpha_1$ and $\alpha_2$ were set to 0.5 for simplicity. Figure 3(b) shows the noise figure as a function of the duty cycle and the input power to the optical gate. The results reflect that a decreased duty cycle introduces high losses in the parallel path and degrades the OSNR performance of the drop and extract operation. Consistent with the dominance of noise generated in amplifier $G_3$, the OSNR degradation is inversely proportional to the gate launch power. For a signal input power of 0 dBm, OSNR reaches to 39 dB for a duty cycle of $d = 0.2$ and a gate input power of 12.5 dBm, both readily achievable using lithium niobate modulators.

### *3.2. Optimization of optical gating process*

For the numerical evaluation of the node performance we have considered a drop, extract and insert scenario of a single sub-channel from the OFDM super-channel. The OFDM signal comprised seven optical sub-carriers of 10 GHz frequency spacing. The sub-carriers were modulated independently in NRZ-BPSK format using Mach-Zehnder modulators, driven by 10 Gbit/s randomly generated binary sequences of rectangular pulses (1's and 0s of equal probability). The electrical signals experienced also the low pass response of a 1st order Gaussian filter, which gave them a rise-time of 10 ps. In this paper, the combination of filters and pulse shape used did not satisfy the zero ISI orthogonality condition, so instead of adding a time or frequency guard interval, the phase difference between the adjacent sub-carriers was fixed at $\pi/2$ [22]. The simulation bandwidth was 1.28 THz.

The WSS units that performed the super-channel selection were simulated with a 3$^{rd}$-order Gaussian transfer function of 100 GHz 3-dB bandwidth. For the modelling of the FFT/i-FFT filters we assumed either an ideal sinc$(fT)$ shape or a LCoS based photonic spectral processor (PSP) [23, 24], using the predicted frequency response of this device technology [25]. We assumed a rectangular switching window synchronized to the de-multiplexed pulse-stream for the optical gate allowing the switching window and contrast ratio to be independently varied. Signals were detected using an optically pre-amplified coherent receiver with a zero linewidth local oscillator (to allow us to focus on the impact of the node) and an FFT optical demultiplexing filter. The performance was quantified by an iterative Monte-Carlo method [26] with direct error counting. Iterations were performed using each time different random binary patterns of $2^{15}$ bit-length for the OFDM sub-channels and they were terminated when the BER estimation was statistically expected to have less than 10% error, i.e. when a total of $\sim 100$/BER bits were simulated [27]. The impact of each degradation was assessed by calculating the corresponding receiver sensitivity penalty (defined at BER=$10^{-4}$) at the output of the node with respect to the back-to-back performance.

Figures 4(a) and 4(b) show the results of the gating optimization where to concentrate on the inter sub-channel crosstalk, we assumed ideal i-FFT/FFT filters and no ASE induced noise from the amplifiers in the node. Figure 4(a) shows the sensitivity penalty as a function of the switching window for ch 4′ and its two immediate neighbors (ch 3 and ch 5) assuming ideal contrast ratio. Ch 4′ is the most affected channel since it experiences in-band crosstalk from sub-optimal gating. The penalty remains below 0.2 dB for the three channels when the switching window is kept below 17 ps. For longer switching periods ($>$30 ps) a rapid increase in the penalty has been calculated for ch 4′ ($>$1.2 dB). For the other two channels that bypass the node the impact is greatly reduced and the penalty does not exceed 0.3 dB resulting solely from the crosstalk due to the residual ch 4 components. Practical gates [15–17] have a limited contrast ratio which is expected to introduce additional degradations in the system performance. Figure 4(b) shows the sensitivity penalty as a function the gate contrast ratio for a rectangular switching window of 12 ps. Compared to the results of Fig. 4(a) the impact here is more detrimental. The contrast ratio should be kept higher than 24 dB to ensure penalty less than 1 dB. Decreasing this

#227008 - $15.00 USD Received 17 Nov 2014; revised 11 Feb 2015; accepted 11 Feb 2015; published 25 Feb 2015

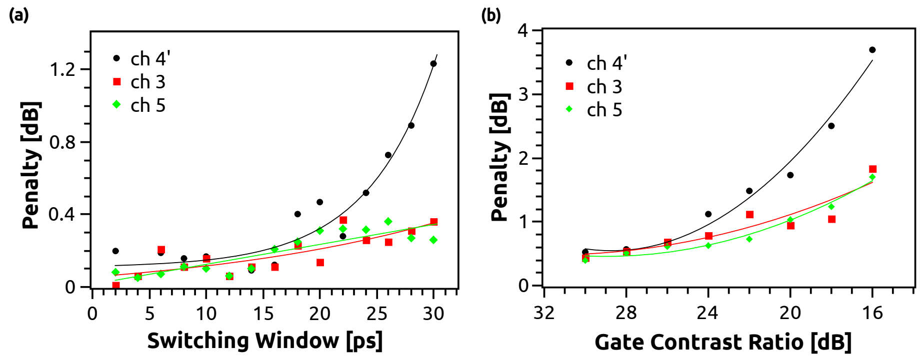


Fig. 4. Sensitivity penalty for the added sub-channel (ch 4′) and its two neighbors (ch 3, ch 5) as a function of (a) the switching window assuming ideal contrast ratio and (b) the contrast ratio of the optical gate assuming switching window of 12 ps.

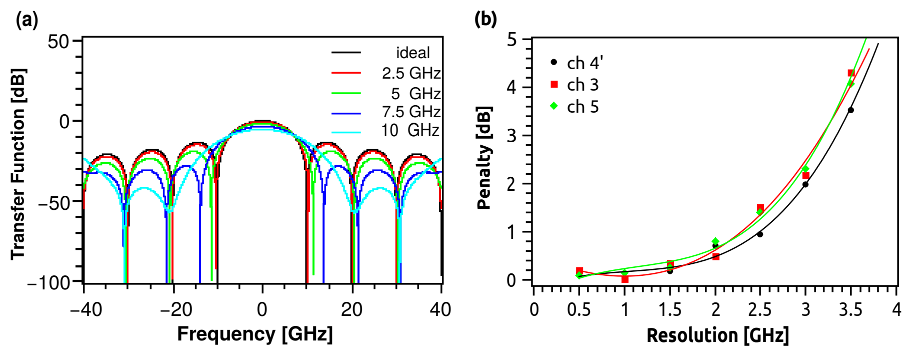


Fig. 5. (a) Transfer function of sinc-shaped FFT filters implemented by optical spectral processors of different resolution parameters; (b) Sensitivity penalty of added channel (ch 4′) and its two neighbors (ch 3, ch 5) as a function of the resolution of the photonic spectral processors that implement the FFT/i-FFT filtering in the node and at the receiving end.

parameter below 24 dB leads to a rapid increase of the penalty due to incomplete suppression of the crosstalk, which is itself reshaped by the FFT and therefore constrained to degrade the extract operation. Consequently, for ch 3 and ch 5 the penalty is significantly lower and does not exceed 2 dB.

### *3.3. Impact of FFT/i-FFT filter resolution*

For the simulations of Fig. 4 ideal FFT/i-FFT filters were considered. In reality, the limited spectral resolution of the PSP, will have an impact on the actual frequency response. Based on spatial filtering of the spectrally dispersed light, as occurring in WSS and calculating the overlap integral [25], we identified the closest achievable approximation to the sinc$(fT)$ function for various spectral resolution metrics (in GHz) of the spectral processor (defined as the spot size of a single frequency component (in m) divided by the spatial dispersion (in m/Hz)). A selection of frequency responses is shown in Fig. 5(a) where resolutions courser than 5 GHz (i.e. $2/T$) flatten out the sinc response reducing the accuracy of the FFT. As a result crosstalk is introduced, which we expect to degrade the overall performance. We have numerically in-

#227008 - $15.00 USD Received 17 Nov 2014; revised 11 Feb 2015; accepted 11 Feb 2015; published 25 Feb 2015

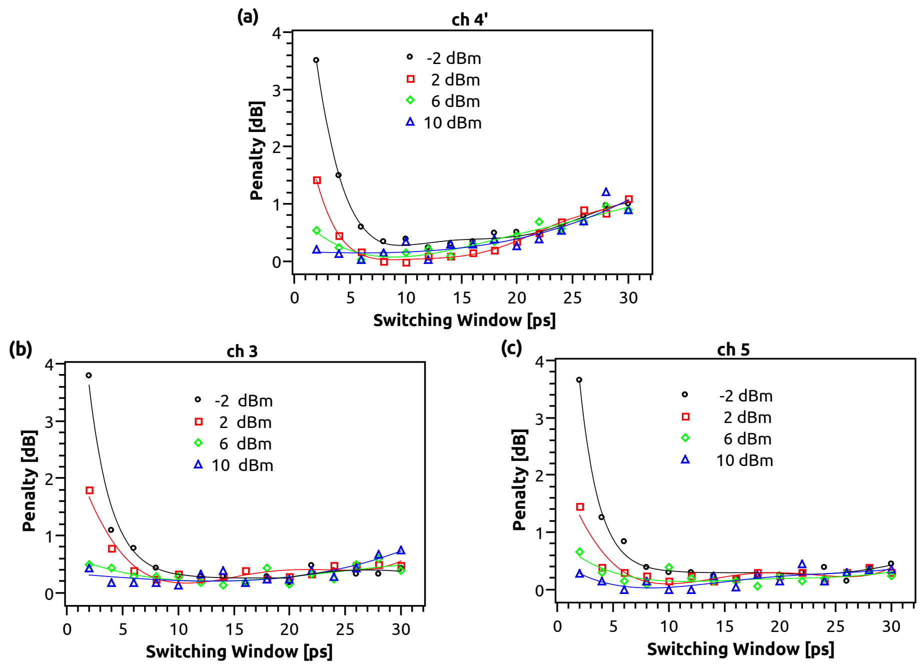


Fig. 6. Penalty for (a) ch 4′, (b) ch 3 and (c) ch 5, as a function of the switching window for different power levels $P_g$ entering the optical gate.

vestigated the impact of the limited PSP resolution on the switching performance of the node. Fig. 5(b) shows the sensitivity penalty for the three channels under study. The results have been taken ignoring the generation of ASE noise from the amplifiers in the node and considering the optical gate with high contrast ratio (30 dB) and 12 ps switching window. The impact of PSP resolution has been considered for both of the FFT/i-FFT filters in the parallel path (branch B) and also for the FFT-demultiplexer at the receiving end. To maintain a sensitivity penalty below 0.5 dB finer resolutions than 1.5 GHz are needed. A PSP device capable of that performance has been recently demonstrated in [28]. For coarser resolution values the penalty grows rapidly above 1 dB and for the three channels.

### *3.4. Overall performance analysis*

Finally, we have included the effects of the ASE filtering emitted by the optical amplifiers in the node and we have numerically investigated the trade-off between the OSNR degradation and the inter-symbol interference introduced by the gating process. Fig. 6(a), 6(b) and 6(c) show the penalty for the added channel (ch 4′) and its two neighbours (ch 3, ch 5) as a function of the switching window and for different power levels launched at the input of the gate $P_g$, for a PSP resolution below 1 GHz and a gate contrast ratio higher than 30 dB. For the added channel (ch 4′), the sensitivity penalty remains below 0.6 dB when the switching window is between 10 to 20 ps. As observed in Fig. 4, for excessive switching window durations the penalty increases more rapidly for the inserted channel (ch 4′) than for its two neighbours (i.e. ch 3 and ch 5). In this switching regime, the impact of the OSNR degradation due to the sampling process is minor and it is unaffected by the input power level to the optical gate. For switching windows shorter than 8 ps the OSNR degradation dominates the performance and

#227008 - $15.00 USD Received 17 Nov 2014; revised 11 Feb 2015; accepted 11 Feb 2015; published 25 Feb 2015

introduces significant penalties to all of channels under study. However, a proper selection of the optical gate technology (e.g. [17]), tolerant to high input powers (>6 dBm), should enable net sensitivity penalties lower than 0.6 dB.

## 4. Conclusion

A novel optical add-drop architecture for OFDM signals has been introduced and an in depth numerical evaluation of its performance has been carried out. Based on purely all-optical processes, i.e. FFT/i-FFT filtering and time domain sampling the scheme may replicate the waveform of any sub-channel and enable its interferometric extraction from the OFDM signal. We have investigated the main degradation factors of the scheme and specified critical device and sub-system parameters, gating width and extinction ratio and PSP resolution. The study was performed considering a 7-channel BPSK modulated OFDM signal with a sub-channel symbol-rate of 10 Gbaud. For the optical gate a contrast ratio higher than 30 dB and a switching window of between 10 and 20 ps is required to achieve adequate performance. Due to noise enhancement effects, the launched power to the gate should exceed 6 dBm. Furthermore, the resolution of the photonic processor for the FFT/i-FFT functionality should be finer than 1.5 GHz.

## Acknowledgments

This work has been supported by the Marie Currie - IEF project ARTISTE (IEF 330697), and the EU-ICT project FOX-C (grant number 318415).